SEASONAL CLIMATOLOGY OF TIDAL NON-LINEARITIES IN A SHALLOW ESTUARY

David G. Aubrey and Carl T.Friedrichs
Woods Hole Oceanographic Institution
Woods Hole, MA 02543

ABSTRACT

Hourly sea levels recorded over a 16-month period at eight tide gauges throughout the estuarine system at Murrells, South Carolina, clarify the climatology of tidal distortion within this shallow, well-mixed estuary. Numerical results are consistent with these data and suggest comparable behavior in other geometrically-similar systems. The non-linear tidal response to changes in the amplitude-to-depth ratio (a/h) are investigated utilizing the spring-neap cycle over a single month and the offshore steric response over an entire year or more. As a/h increases in Murrells estuary due to greater tidal amplitude, tidal distortion becomes more flood dominant. However, patterns of non-linear tidal distortion in response to lower frequency ocean level change are strongly dependent upon proximity to local concentrations of intertidal flats. In areas of small tidal flat extent, as a/h decreases (due to rising sea level), tidal distortion becomes less flood dominant; in areas of extensive flats, absolute distortion and, therefore, flood dominant nature grows with greater h. Numerical modeling of estuary sea height and tidal velocity support the observations, which are consistent with the hypotheses of Aubrey and Speer (1985) and Speer and Aubrey (1985). They also have implications for changes in estuarine response to accelerated sea-level rise in the near future.

INTRODUCTION

If present trends continue, global mean sea level has been predicted to rise 144 to 217 cm over the next century due to climate change (NRC, 1983; Hoffman et al., 1983). Among the first environments to show clear effects of encroaching seas will be estuaries. Estuarine coastlines (lagoons, bays, inlets, tidal flats, and marshes) make up 80-90% of the U.S. east and Gulf of Mexico coasts and occur on every continent (Emery, 1967). Estuarine systems play a significant role in the sediment cycle, transporting material between land and sea and often acting as major sediment sinks. Although the potential impact of rising sea level on the human concerns of accelerated coastal development is formidable, the initial effects of increases of less than a meter remain, by and large, unresolved.

Yet the impact of sea-level rise on the order of tens of centimeters can be observed directly in temperate zones utilizing the seasonal sea-level response to changing water density (steric response). Offshore of the tidal inlet and estuary at Murrells, South Carolina (Figure 1), mean monthly sea level varies approximately 30 cm. Up to a year-and-a-half of

Lecture Notes on Coastal and Estuarine Studies, Vol. 29
D.G. Aubrey, L. Weishar (Eds.), Hydrodynamics and Sediment Dynamics of Tidal Inlets

continuous sea surface elevation data from eight tide gauges spaced throughout the estuarine system enable the examination of tidal distortion under a variety of oceanographic and climatological conditions. Changing conditions analogous to the sea-level rise predicted over coming decades produce significant variations in tidal distortion in estuaries and therefore expected sediment transport patterns.

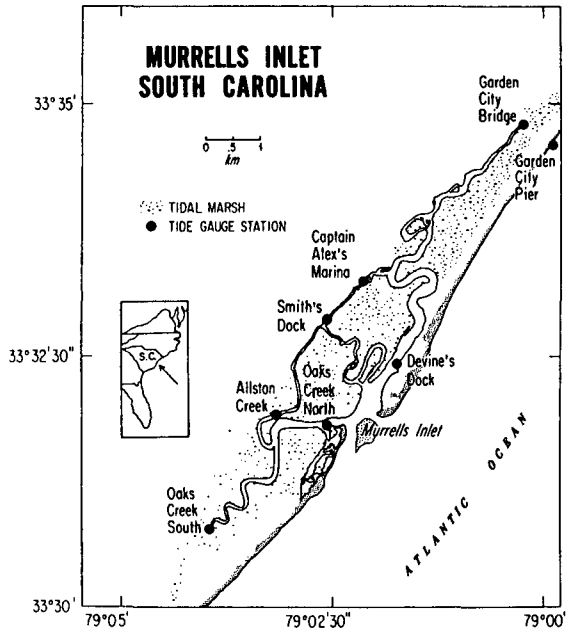

Figure 1. Location map of inlet and channels at Murrells, South Carolina, showing placement of National Ocean Survey tide gauges. The study was performed prior to stabilization of this inlet.

The flood and ebb of a tide in a coastal inlet, lagoon, or bay usually are distorted in duration, height, and velocity. The importance of these asymmetric cycles in the transport and accumulation of sediment in shallow estuaries is well established (e.g., Postma, 1967; Boothroyd, 1969; Aubrey, 1986). If sediment in a well mixed tidal channel has a transport rate non-linearly related to velocity, then net transport still may occur without residual tidal flow (Aubrey, 1986; Fry, 1987). "Flood dominant" systems (having shorter duration, higher velocity floods) tend to infill their channels with coarse sediment. "Ebb dominant" estuaries (having shorter duration, higher velocity ebbs) tend to flush bed-load sediment seaward more effectively and may represent more stable geometries. Strongly flood dominant systems are typically shallow (relative to tidal amplitude) having only small-to-moderate storage capacity in intertidal flats and marshes. Such systems become relatively more ebb dominant with increased depth, decreased tidal amplitude, or increased intertidal storage area (Aubrey and Speer, 1985; Friedrichs and Aubrey, in press).

The distortion of the tide as it propagates from the open ocean to the confinement of estuaries can be represented by the non-linear growth of compound constituents and harmonics of the principal astronomical tidal components (e.g., Dronkers, 1964; Aubrey and Speer, 1985). Transfer of energy to even harmonics can produce distortion in tidal velocity and net sediment transport of coarse bed load sediment. As shown by Fry (1987), distortions in tidal height at the landward end of a tidal channel place continuity constraints on distortions in tidal velocity. Where direct measurements of tidal velocities are unavailable, observations of harmonic components of tidal height can provide a useful first approximation of net sedimentation patterns. By utilizing system geometry and sea surface data, one-dimensional numerical modeling can be used effectively to predict velocity trends. The most dominant astronomical constituent off Murrells Inlet is M_2 (Figure 2a), the semi-diurnal lunar tide. Because of M_2 dominance, the most significant overtide formed within the lagoon is M_4, the first harmonic of M_2. The non-linear transfer of energy to other quarter-diurnal components is similar (Aubrey and Speer, 1985). The comparable influences on tidal distortion of the three largest quarter-diurnal components is illustrated by their similar relative sea surface phases within the estuary at Murrells (Figure 2b). Thus nature of tidal distortion in the Murrells estuarine system can be represented well by analyzing M_4 and M_2 interactions alone.

According to simple harmonic motion,

$$A = a_{M_2}\cos(\omega t - \theta_{M_2}) + a_{M_4}\cos(2\omega t - \theta_{M_4})$$

$$V = v_{M_2}\cos(\omega t - \phi_{M_2}) + v_{M_2}\cos(2\omega t - \phi_{M_4})$$

where t is time, ω is tidal frequency, a is amplitude of tidal height, v is amplitude of tidal velocity, θ is phase of tidal height, and ϕ is phase of tidal velocity. Thus the distorted, composite sea surface height and tidal velocity are given at any time by A and V. The sea surface phase of M_4 relative to M_2 is defined as

$$2M_2 - M_4 = 2\theta_{M_2} - \theta_{M_4}$$

A direct measure of non-linear distortion, the M_4 to M_2 sea surface amplitude ratio, can be defined as

$$M_4/M_2 = a_{M_4}/a_{M_2}$$

Likewise the non-linear parameters for tidal velocity are $2\phi_{M2}$-ϕ_{M4} and v_{M4}/v_{M2}. An undistorted, symmetric tide has M_4/M_2 amplitude ratios of zero. If M_4 is locked in a velocity phase of -90 to 90 degrees relative to M_2 with $M_4/M_2 > 0$ (Figure 3a), the distorted composite tide has a higher velocity flood and is defined as flood dominant. Assuming a linear relationship, a flood dominant system has a sea surface phase of 0 to 180 degrees (Figure 3b). If M_4 is locked in a velocity phase of 90 to 270 degrees and a surface phase of 180-360 degrees, the relationship is reversed, resulting in an ebb dominant system. In either case, the larger the M_4/M_2 ratio, the more distorted the tide and the more strongly

flood or ebb dominant the system becomes. The system at Murrells, with a $2M_2$-M_4 relative surface phase ranging from about 80 to 110 degrees, is flood dominant (Boon and Byrne, 1981).

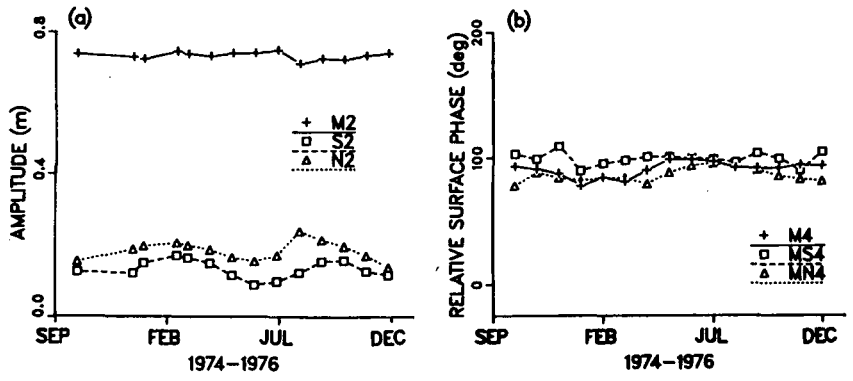

Figure 2. Murrells, S.C., averages over 29-day cycles: (a) Amplitudes of the three most significant semi-diurnal tidal components at the Garden City Pier ocean gauge. (b) Sea-surface phases (relative to their source components) of the three most significant quarter-diurnal tidal components at the Garden City tidal channel gauge. M_4, MS_4, and MN_4 are formed by the non-linear interaction of the three largest semi-diurnal components, M_2, S_2, and N_2.

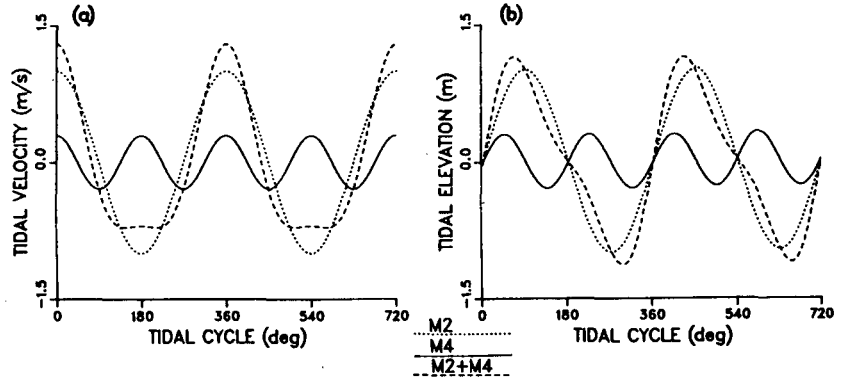

Figure 3. Model of a flood dominant (stronger flood flow) distorted tide: (a) M_4/M_2 velocity ratio = 0.3, $2M_2$-M_4 relative velocity phase = 0°, (b) M_4/M_2 sea surface amplitude ratio 0.3, $2M_2$-M_4 relative surface phase = 90°.

The conditions at Murrells are favorable for the study of non-linear tidal distortion. The estuary has a well-mixed water column and receives little surface runoff. It contains two independent major channels that provide control for testing the effects of varying system geometry on tidal distortion. Furthermore, advantageous placement of tide gauges allows the examination of changes in tidal asymmetry along the length of individual channels. Finally, a year-and-a-half of tide-gauge data are available for Murrells (including four stations previously analyzed for two months in Boon and Byrne, 1981), providing the opportunity to observe tidal distortion under a range of oceanographic and climatological conditions.

Murrells is located 32 km northeast of Georgetown, South Carolina, and 22 km southwest of Myrtle Beach, South Carolina, on the eastern edge of the Southern Atlantic Coastal Plain along the south flank of the Cape Fear Arch. In the vicinity of Murrells, pre-Mesozoic crystalline basement rock of the Piedmont are overlain by 2000 feet of unconsolidated and semi-consolidated wedges of Mesozoic and Cenozoic coastal-plain sediments that thicken and dip gently eastward (Richards, 1974). The inlet and estuary at Murrells are located entirely in unconsolidated Holocene barrier and backbarrier deposits of the Waiter Island Formation (Dubar et al., 1974). At the time all field data were collected, an unimproved inlet provided access through beach and dune sands to a well-mixed tidal estuary of ocean salinity that has no source of fresh water inflow other than local surface runoff (Perry et al., 1978). The estuary consists of a salt marsh intersected by two major tidal channels and several smaller tributaries. The major channels are between four and eight kilometers in length and more or less adjacent to areas of extensive tidal flats. The tide seaward of Murrells is predominantly semi-diurnal having a range of approximately 1.6 meters, suggesting that finite amplitude effects (tidal amplitude/channel depth>>0) will be a significant source of tidal distortion in the estuary. The channels are also long in comparison to their width, and the horizontal aspect ratio is small (channel depth/width<<1). The flow therefore may be termed one-dimensional although channel bends visible in Figure 1 will produce locally two-dimensional effects.

The present study evolved from work in the tidal inlet and estuary of Nauset, Massachusetts (Aubrey and Speer, 1985; Speer and Aubrey, 1985). Field measurements of tidal distortion at Nauset were used to develop a one-dimensional numerical model of the kinematics and mechanics of shallow estuarine tidal distortion. The modeling did not attempt to reproduce the exact conditions at Nauset. Estuarine systems such as Nauset are physically too complex and require at least two-dimensional modeling to predict precisely sea surface levels. Such two-dimensional models exist (e.g., Masch et al., 1977), and these numerical models more accurately reproduce lateral variations in estuarine circulation. This lateral dependence is critical for precise predictions of particle pathways, but less important for defining general system response of small-scale, shallow, well-mixed estuaries. Once the general system response is identified, more complex modeling can be used eventually to refine the results. By utilizing the one-dimensional equations of motion,

the Speer-Aubrey model produces computer model runs of more reasonable cost and duration. More importantly, because the inputs to the Speer-Aubrey model may be adjusted quickly, it can examine easily the roles of the parameters that actually control tidal distortion.

METHODS

Data Analysis

In 1971, the U.S. Army Engineer District, Charleston (SAC), submitted recommendations for the improvement and stabilization of Murrells Inlet (Perry et al., 1978). In anticipation of constructing a concrete scale-model of the estuary, comprehensive bathymetric data were obtained by SAC from March to May 1974 (Figure 4). In conjunction with NOAA National Ocean Survey, SAC placed eight tide gauges (Table 1) in and around the inlet and lagoon at Murrells between September 1974 and March 1977 over intervals ranging from four to thirty months (NOS, 1984). The sea surface elevations, originally sampled every six minutes, were resampled at hourly intervals before being stored by NOS in the Tides Automated Login and Retrieval Systems.

The method of least squares harmonic analysis was used to extract tidal components from the sea surface data recorded at Murrells. For the least squares method, no requirements are placed on the length of the sea surface record nor on the sample interval (Speer and Aubrey, 1985). However, tidal records extending over one full lunar rotation (697 hours) are convenient for approximating stable values of constituent amplitudes. For sufficiently continuous series of 697 hourly observations at Murrells, twenty-nine tidal constituents were extracted (beginning approximately every 15 days). For 73-hour series (beginning every 40 hours) which were utilized for the study of tidal variation over a single month, only four of the major components were extracted because of limitations in accuracy and resolution.

Geometric analysis of the estuary at Murrells was accomplished utilizing data from the detailed bathymetric map (contour interval of two feet) charted by SAC a few months before the tide-gauge data collection. To quantify geometric constraints on channels at Murrells, the lagoon was divided into southern and northern systems based upon the drainage patterns depicted on the SAC bathymetric map. This division is justified in that the interaction between the two main tidal channels is minimal (Figure 4). "Tidal flats" refer to the unvegetated areas adjacent to the channels that are exposed between mean high and mean low tides. Flats are shown on the SAC map as unshaded regions between the zero contour (low water) and the edge of vegetation. Areas below the zero contour are classified as "channels".

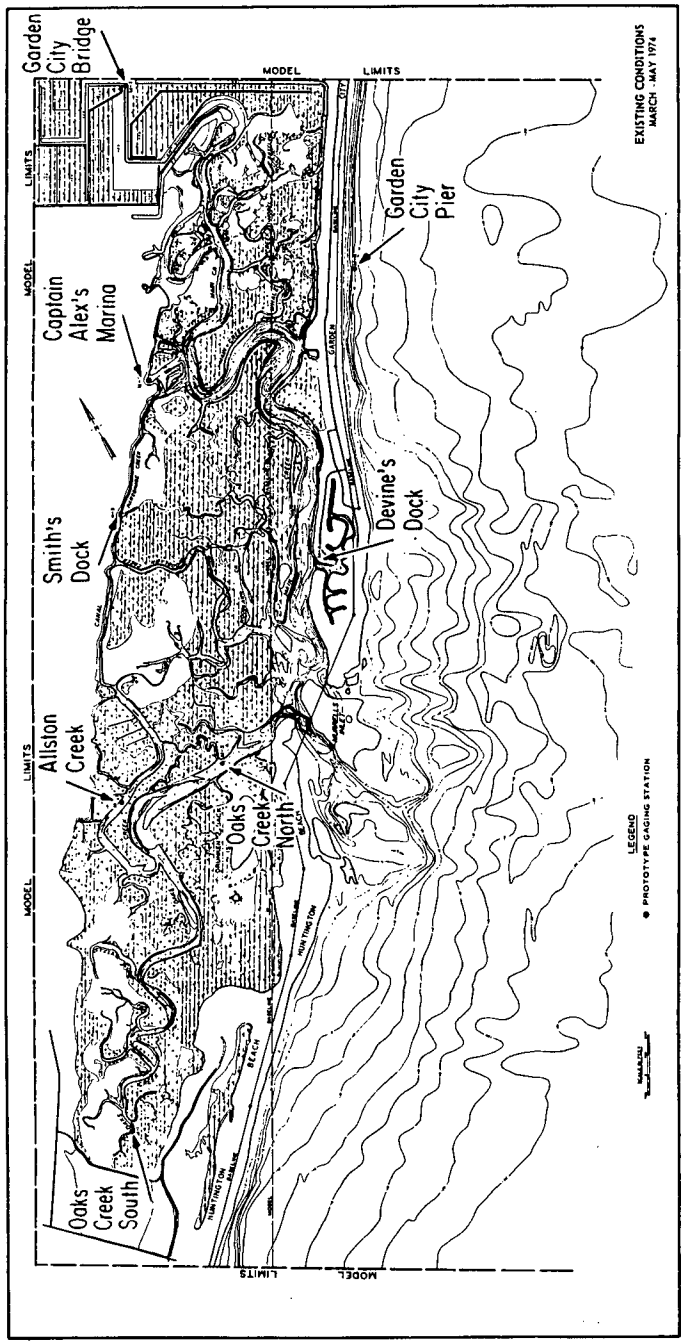

Figure 4. Bathymetric map of Murrells locale made by the U.S. Army Engineer District, Charleston, prior to placement of tide gauges. Tide gauge locations have been added for clarity. Tidal flats are shown as unshaded regions grouped primarily at the ends of the main channels. The contour interval is two feet (from Perry et al., 1978).

TABLE 1

Duration of sea-height observations and descriptions of tide gauge locations:

System/Station	Duration of Record	Distance up channel (km)	Depth of channel, h_2(m)
Ocean			
Garden City Pier	10/01/74-10/31/74, 12/16/74-01/31/75, 02/14/75-12/31/75	0.0	--
Northern Channel			
Devines Dock	10/21/74-11/31/74 12/05/74-01/25/75 03/21/75-01/11/76 04/01/76-09/30/76	1.2	3.7
Captain Alex's Marina	10/15/74-12/31/74	4.7	3.7
Garden City Bridge	10/01/74-01/31/76	8.0	0.8
South Channel			
Oaks Creek North	10/01/74-03/31/75 04/06/75-01/31/76	0.8	2.5
Alston Creek	10/01/74-12/31/74 02/01/75-04/30/75	2.9	1.2
Oaks Creek South	10/07/74-01/31/76	4.7	0.9
Other			
Smith's Dock	10/01/74-12/31/74 01/18/75-11/29/75 12/04/75-01/01/76	3.0	1.2

Numerical Analysis

The one-dimensional model of Speer and Aubrey (1985) was used to evaluate trends in tidal distortion at Murrells, South Carolina. The equations of motion on which the model is based are:

$$\text{Momentum equation: } \frac{\partial U}{\partial t} + \frac{\partial}{\partial x}\frac{U^2}{A} = gA\frac{\partial \zeta}{\partial x} - \frac{\tau_b}{\rho}P$$

$$\text{Continuity equation: } \frac{\partial \zeta}{\partial t} + \frac{1}{b}\frac{\partial}{\partial x}U = 0$$

where $\zeta(x,t)$ is the sea surface elevation, t is time, g is the acceleration of gravity, b is channel width, U(x,t) is the cross-sectional flux, τ_b is the average shear stress on solid

boundaries, P is the wetted channel perimeter, A is the channel cross-sectional area, and ρ is the water density. The problem is closed mathematically by formulating friction as:

$$\tau_b = \frac{\rho f |U| U}{A \cdot A}$$

where f is a dimensionless friction factor. Principal non-linear effects in these equations enter through quadratic friction, advection of momentum, and tidal interactions with estuarine geometry in the continuity equation.

The Speer-Aubrey model uses a modified trapezoidal geometry to represent the estuarine channel, where width increases with elevation above the bottom (Figure 5). The model approximates an ideal shallow estuary having two distinct elements: (1) a trapezoidal channel transporting all the momentum of the system and (2) shallow, sloping tidal flats which act in a storage capacity only. By including the tidal flats in just the continuity equation, the strong drop in velocity seen as water flows across tidal flats is approximated. The Speer-Aubrey model assumes a small horizontal aspect ratio, long narrow channels and little fresh water input. Although these criteria may seem limiting, these characteristics are common along over 5000km of navigable waters along the U.S. Atlantic and Gulf of Mexico coasts alone.

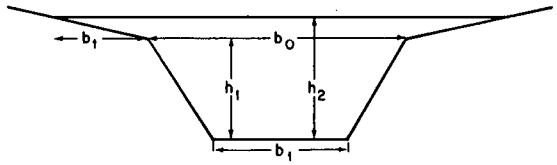

Figure 5. Trapezoidal model of channel geometry with tidal flats included (from Speer and Aubrey, 1985).

b_l = width of channel at its base
b_0 = width of channel at its top
b_t = width of tidal flat
h_1 = depth of channel
h_2 = mean depth of water column

RESULTS AND DISCUSSION

The two parameters that quantify distortion in tidal height (the M_4/M_2 surface amplitude ratio and the $2M_2$-M_4 relative surface phase) exhibit significant changes from the open sea to within the tidal channels at Murrells. The 29-day averaged values for the M_4/M_2 ratio exhibit progressively increasing tidal distortion inland (Figure 6a). Outside the estuary at the Garden City Pier ocean (outer) gauge, M_4/M_2 seldom rises above 0.01; within the estuary, at the Garden City Bridge inner tide gauge, M_4/M_2 climbs ten-fold to over 0.1. At the Garden City Pier outer gauge, monthly magnitudes for $2M_2$-M_4 relative phase vary widely (Figure 6b). Because of this relative phase variation and the near zero values for M_4 amplitude on the ocean at Garden City Pier, the ocean/estuary $2M_2$-M_4 relative phases are assumed to be decoupled. Within the estuary the $2M_2$-M_4 relative

phases are concentrated near 90 degrees, showing the tidal channels at Murrells to be flood dominant (Aubrey, 1986; Friedrichs and Aubrey, in press).

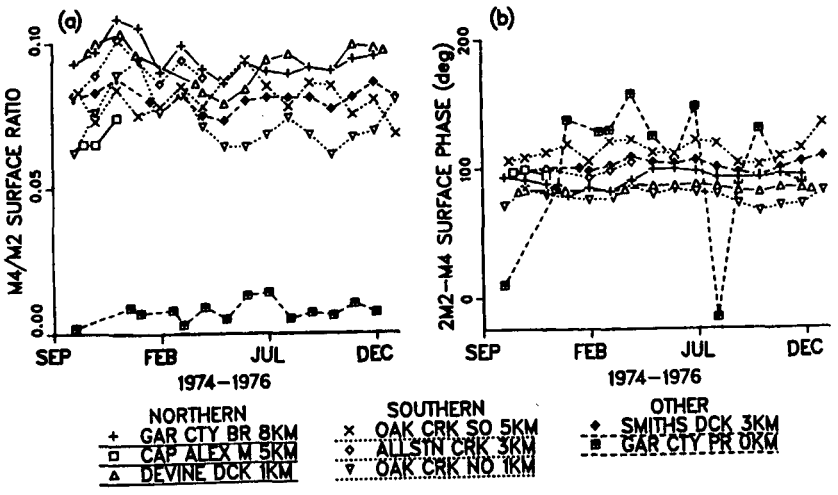

Figure 6. Murrells, S.C., averages over 29-day cycles at all eight tide gauges: (a) M_4/M_2 sea-surface amplitude ratios. (b) $2M_2$-M_4 relative sea-surface phases.

The tide at the head of the primary northern channel exhibits a shorter sea surface M_2 phase lag and a smaller drop in M_2 amplitude than at the head of the primary southern channel (Figure 7a). The tide is also more strongly flood dominant at the head of the northern channel as expressed by a larger M_4/M_2 sea surface ratio and a smaller $2M_2$-M_4 relative surface phase (i.e., farther from a symmetric 180 degrees). The primary northern channel is 73% deeper and 72% longer than the primary southern channel (Table 2). If channel length were the most important parameter determining differences in tidal distortion at Murrells, the M_2 phase lag would be greater in the northern channel, which is not the case. If channel depth were most important, the northern system would be least flood dominant. Greater depth (lower a/h) favors reduced distortion because tidal interaction with the channel bottom is decreased. Therefore the intertidal storage capacity (ratio of area of tidal flats to channel area--A_f/A_c) of the two main systems may be the most significant distinguishing feature. One-dimensional modeling also indicates that differences in A_f/A_c can cause the patterns of tidal distortion seen at Murrells (Figures 7b, 7c). The models utilize the average geometry of the two main tidal channels at Murrells and differ only in extent of tidal flats. The A_f/A_c values for the two models--0.68 and 1.82--are identical to the A_f/A_c values of the northern and southern systems at Murrells. The $2M_2$-M_4 relative sea-surface phases are less than 180 degrees, and the relative velocity phases are between -90 and 90 degrees for both the channels. Therefore these model systems contain shorter floods with, necessarily, higher velocities. Also like the tidal channels at Murrells, the

model system having more tidal flats exhibits a tide with a greater M_2 sea surface phase lag and a larger drop in M_2 surface amplitude. This occurs because the rise and fall of the tide is dampened and delayed by the filling and emptying of water stored in the tidal flats. M_2 velocity is greater in the model system with more water in intertidal storage because it transports a larger volume of water in the same sized channel.

Consistent with field results, the model channel adjacent to greater tidal flats is less strongly flood dominant, as expressed by generally lower M_4/M_2 ratios, a higher $2M_2$-M_4 surface phase, and a $2M_2$-M_4 velocity phase further from zero degrees. Greater tidal flats extent decreases flood dominance (increases relative ebb dominance) because the tidal wave propagates less efficiently across very shallow tidal flats than in channels (Boon and Byrne, 1981; Dronkers, 1986; Friedrichs and Aubrey, in press). The turn to ebb takes place later on the flats than in the channels. This leads to a strong water inclination and relatively higher velocity ebb currents.

The model values do not match precisely those values measured in the field. Rather, the simplified models are designed only to predict trends as found in field data, based upon the extent of tidal flats in a particular system. The values for both M_4/M_2 and the $2M_2$-M_4 relative phase are significantly less flood dominant at Captain Alex Marina (4.7km) than at the other tide gauges along the northern channel (Figure 7a). This particular tide-gauge station was positioned adjacent to a relatively large expanse of intertidal flats (see Figure 4). Consistent with the trends predicted for areas having more extensive tidal flats, drainage off the flat has reduced net tidal distortion locally. Deviations from the expected behavior of M_2 phase and amplitude are not seen at Captain Alex Marina. The localized effect of tidal flats is clearer in the behavior of M_4 because M_4 is formed by non-linear effects within the lagoon. M_2, on the other hand, is an astronomical constituent forced offshore. Differences in channel depth at Murrells may account also for some deviation from model results. In terms of net tidal distortion, the greater depth of the primary northern channel compensates partially for the more extensive flats of the southern system; the non-linear behavior of the two systems is more similar than it would have been if both channels were of equal depth. To examine climatology of the generation of non-linear tides caused by varying a/h, day-to-day variability in distortion was analyzed. Tidal sea surface amplitude, averaged over three day periods, varies on the order of 50 cm over the spring-neap cycle at Murrells, whereas monthly mean tidal amplitude fluctuates by only 5 cm. On the other hand, fluctuation in mean sea level during a single month (less than 15 cm) is not as great as that seen over the entire year (over 30 cm). By examining non-linear parameters over a single month, the effects of changes in forcing amplitude may be studied while minimizing the influence of variations in sea level.

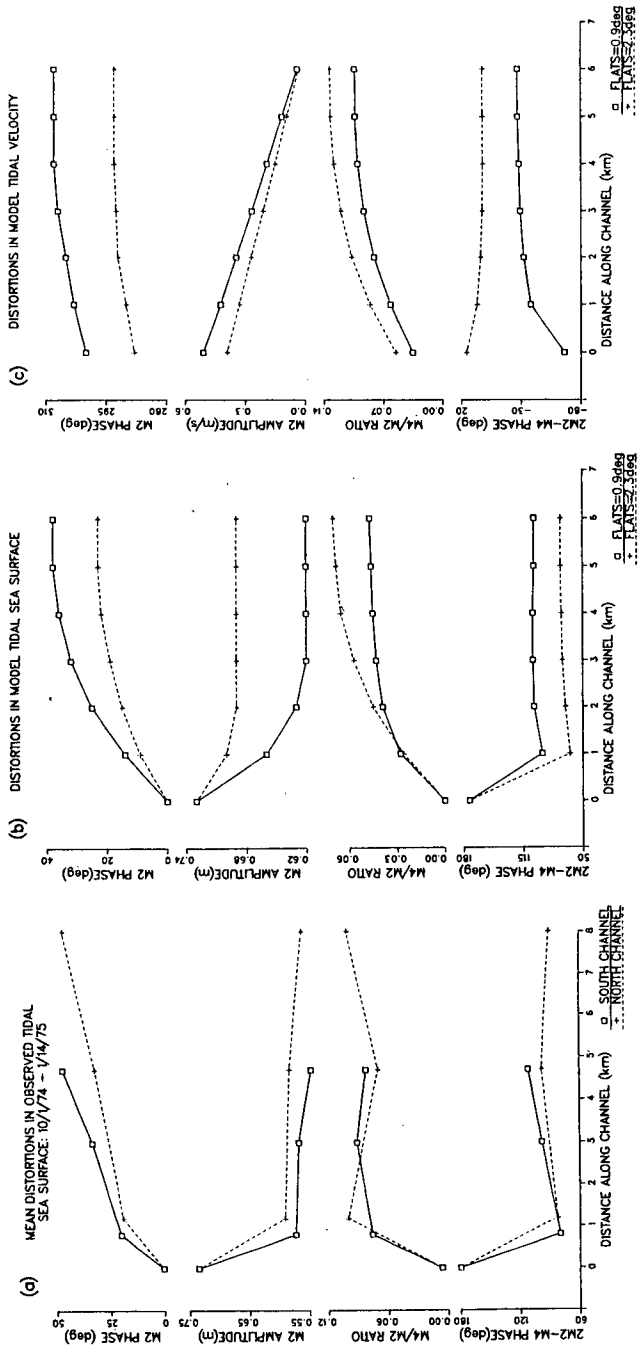

Figure 7. Changes in distortion parameters as a function of distance: (a) Distortion in sea surface along the primary tidal channels at Murrells, S.C. (b) Distortion in sea surface and (c) distortion in velocity along two model channels differing only in extent of tidal flats (b_0=108m, b_1=59m, h_1=1.9m, h_2=2.6m, l=6.5km).

TABLE 2a

NON-DIMENSIONAL GEOMETRIC PARAMETERS AT MURRELLS:

	a/h	$\Delta b/b_o$	A_f/A_c
NORTHERN SYSTEM	0.29	0.48	0.68
SOUTHERN SYSTEM	0.40	0.41	1.82

(Mean M_2 amplitude at Garden City Pier ocean gauge = 0.73 m)

TABLE 2b

MEAN CHANNEL MEASUREMENTS:

(km)	b_1(m)	b_o(m)	h_2(m)	LENGTH
NORTHERN CHANNEL, MURRELLS, S.C.	65	125	3.0	8.0
SOUTHERN CHANNEL, MURRELLS, S.C.	53	90	2.2	4.7
AVERAGE USED FOR 1-D MODEL CHANNEL	59	108	2.6	6.4

Linear regression clarifies relationships between potential causes of changes in tidal distortion (namely amplitude and sea level) and the parameters which quantify non-linear tidal distortion (M_4/M_2 and $2M_2$-M_4 phase). May 1975 was chosen to represent the effects of amplitude variation because mean sea level was relatively constant during that month. The probability that the best-fit coefficient is of the same sign as the true coefficient was determined using the t-test (Table 3). Increases in M_2 tidal amplitude on the open sea due to the spring-neap cycle clearly produce a rise in the sea surface M_4/M_2 ratio within the tidal channels of Murrells (Figure 8a). The trends are similar for both of the primary channels. The data also suggest that as open sea M_2 amplitude increases, estuarine $2M_2$-M_4 relative surface phase declines (Figure 8b).

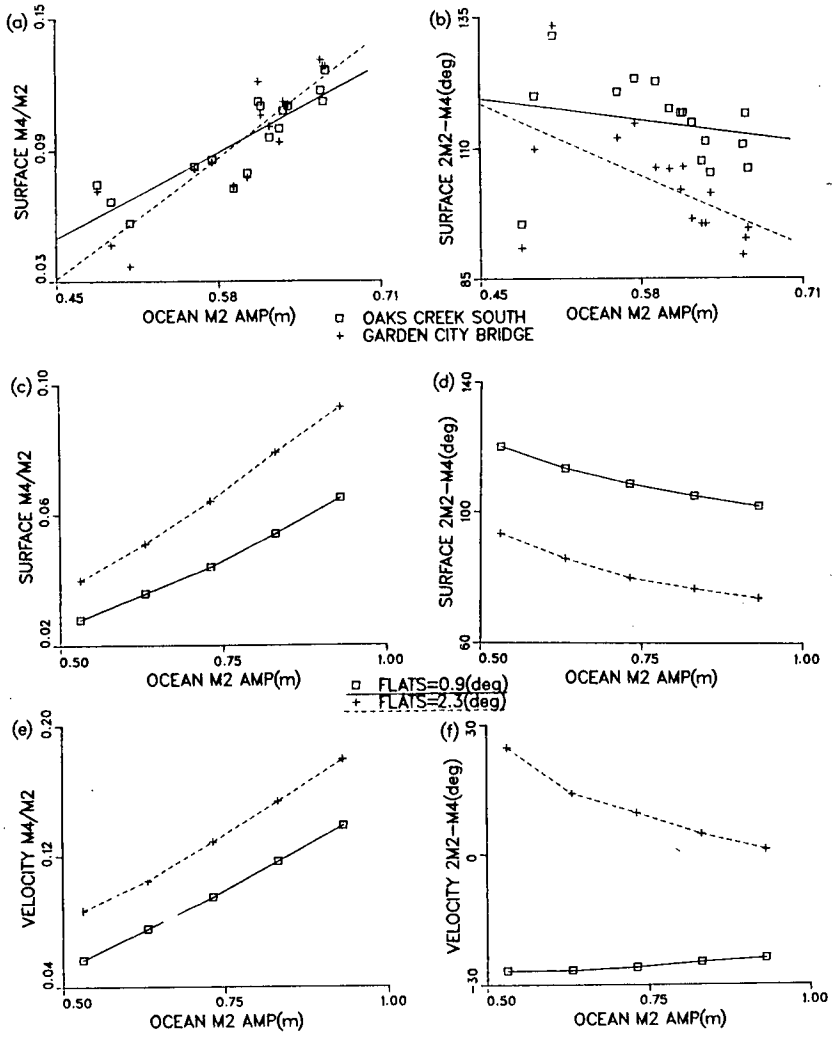

Figure 8. Distortion parameters as a function of ocean M_2 amplitude: Murrells estuary sea surface averages over 16 73-hour cycles, May 1975, for (a) M_4/M_2 amplitude ratio, (b) $2M_2$-M_4 relative phase. Model results for sea surface (c) M_4/M_2, (d) $2M_2$-M_4 and for velocity (e) M_4/M_2, (f) $2M_2$-M_4. (b_0=108m, b_1=59m, h_1=1.9m, h_2=2.6m, l=6.5km, gauge at 6km).

TABLE 3

Statistical results of t-test relating open ocean M_2 tidal amplitude (a, in meters at Garden City Pier) to M_4/M_2 sea-surface amplitude ratio and M_2-M_4 sea-surface relative phase (at individual stations) for sixteen 73-hour cycles, May 1975; Murrells, S.C.

System:	Ocean	Northern		Southern		Other
Station:	Garden City Pier	Devines Dock	Garden City Bridge	Oaks Creek North	Oaks Creek South	Smiths Dock
M_4/M_2 vs. M_2 amplitude						
best fit slope	-.21	.48	.43	.38	.30	.42
level of probability of sign	999.	.9995	.99995	.9995	.9995	.99995
M_2-M_4 phase vs. M_2 amplitude						
best fit slope	244.	35.8	-104.	-220.	-30.5	-103.
level of probability of sign	0.74	.74	.99	.81	.78	.90

Trends produced by changes in amplitude in the Speer-Aubrey one-dimensional numerical model (Figures 8c, 8d, 8e, 8f) are consistent with those recorded in the field. As earlier, two model tidal channels were used whose geometries are the average of those of the two primary channels at Murrells, differing only in extent of intertidal flats. For these channels, the distortion parameters were recorded 6km upstream from the open ocean. Model results indicate that as M_2 amplitude on the open sea rises, M_4/M_2 for both sea surface and velocity increase (Figures 8c, 8e). The increased interaction between tide and channel enhances absolute tidal distortion and the flood dominant nature of the estuarine systems. Consistent with increased flood dominance, $2M_2$-M_4 velocity phase moves toward zero degrees in each model channel (Figure 8f). The model results suggest a nonlinear relationship between velocity relative phase and sea surface relative phase (Figure 8d). As a/h increases in the model channel with a lesser extent of tidal flats, $2M_4$-M_2 surface phase decreases continually to below 90 degrees, even though greatest distortion of tidal height occurs at 90 degrees. This trend also is observed in the field data at Garden City Bridge and at Oaks Creek North. Field data and one-dimensional numerical model results from shallow systems such as Murrells suggest that the smaller the surface $2M_2$-M_4 relative phase is (i.e. the farther from a symmetric 180 degrees), the more flood dominant the system (Friedrichs and Aubrey, in press).

To examine the impact of varying a/h on tidal distortion, one can also focus on time-varying sea-level height. The seasonal variation in sea level, due primarily to water density changes offshore, is significant at Murrells, whereas monthly changes in tidal amplitude are small (Figure 9). The use of monthly means minimizes the influence of varying spring and neap tidal amplitudes on tidal distortion. Furthermore, relative changes

in tidal amplitude from month-to-month within the estuary channels at Murrells may not be related directly to changes in offshore amplitude.

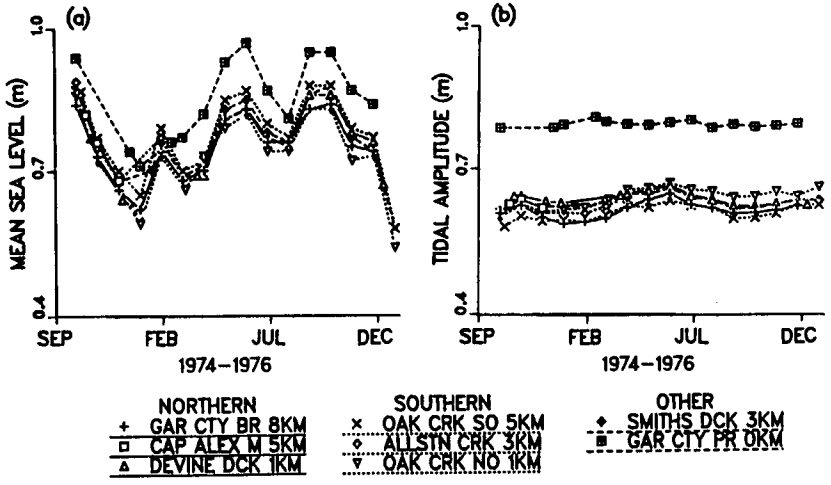

Figure 9. Averages over 697-hour cycles for all eight tide gauges, Murrells, S.C.: (a) Mean sea level relative to local mean low water; (b) Mean tidal amplitude.

Linear regression relates $2M_2$-M_4 relative phase and M_4/M_2 within the estuary at Murrells to mean sea level on the open sea (Table 4). Signifcant correlations suggest that the relationship between ocean levels and estuary sea surface M_4/M_2 is generally negative--except for Oaks Creek South (Figure 10a). Again, the general trend is intuitive--as the channels become deeper (a/h declines), the degree of non-linear energy transfer from M_2 to M_4 is reduced. The relationship between ocean level and estuary surface $2M_2$-M_4 relative phase in the northern channel system also is clear: $2M_2$-M_4 phase falls as ocean sea level declines (a/h increases--Table 4). Oaks Creek South once more exhibits an unexpected result (Figure 10b)--h and phase are inversely related ($2M_2$-M_4 surface phase varies directly with a/h). Significant correlations at Oaks Creek South suggest that, at this one station only, higher sea level actually may increase the flood dominant nature of tidal distortion. As h rises (a/h falls) at Oaks Creek South, surface M_4/M_2 grows and $2M_2$-M_4 phase drops (Figures 10c and 10d). The Oaks Creek South tide gauge, located at the head of the southern system, is positioned adjacent to the largest concentration of intertidal flats in Murrells estuary (Figure 5). The unexpected response may reflect the location of the Oaks Creek South station adjacent to such extensive flats.

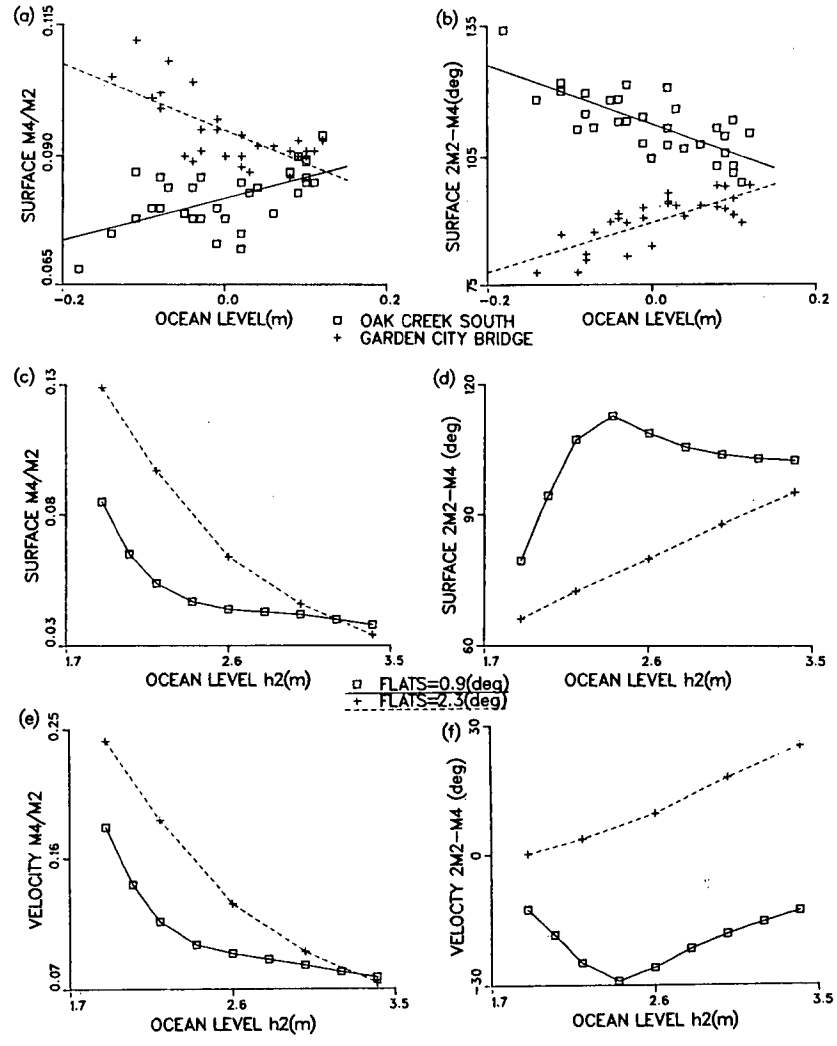

Figure 10. Distortion parameters as a function of mean sea level: Murrells estuary sea surface averages over 697 hour cycles, Oct. '74-Dec. '75, for (a) M_4/M_2 amplitude ratio, (b) $2M_2$-M_4 relative phase. Model results for sea surface (c) M_4/M_2, (d) $2M_2$-M_4, and for velocity (e) M_4/M_2, (f) $2M_2$-M_4. (b_0=108m, b_1=59m, h_1=1.9m, l=6.5km, gauge at 6km.)

Trends produced by Speer and Aubrey's (1985) one-dimensional numerical model due to changes in ocean level again are generally consistent with measurements from the tidal channels at Murrells (Figures 10c, 10d, 10e, 10f). Once more two model channels are used that average the channel geometries at Murrells and differ only in intertidal flat extent. For the model channel having fewer flats, increasing ocean level causes an increase in the estuarine $2M_2$-M_4 sea surface relative phase (as seen along the northern channel at Murrells). For the model system having greater flats, increasing ocean level generally causes a decrease in the estuarine $2M_2$-M_4 surface phase (as seen at Oaks Creek South). At sufficiently low ocean levels the relationship for the extensive flats model is reversed, and it behaves similarly to the model system having fewer flats. Clearly the behavior of the extensive flats model should reverse--at low enough sea level the flats will remain unfilled, effectively leaving a system without flats. Velocity relative phase exhibits a similar pattern (Figures 10c, 10f). In the model channel with fewer flats, as sea level rises, velocity $2M_2$-M_4 increases continuously away from zero degrees. At first $2M_2$-M_4 also moves away from zero in the system with greater intertidal storage. But the trend reverses as ocean level continues to rise. In the two model channels the M_4/M_2 ratio shows a convergence as sea level rises as observed at Oak Creek South and Garden City Bridge, but M_4/M_2 does not actually increase in model runs.

TABLE 4

Statistical results of t-test relating open ocean level (h_2, in meters at Garden City Pier)* to M_4/M_2 ratio and M_2-M_4 relative phase (at individual stations) for 693-hour cycles, October 1974-December 1975; Murrells, S.C.

System:	Ocean	Northern		Southern		Other	
Station	Garden City Pier	Devines Dock	Captain Alex Marina	Garden City Bridge	Oaks Creek North	Allston Creek	Oaks Creek South	Smiths Dock
M_4/M_2 vs. h_2								
best fit slope	.0065	-.045	-.102	-.063	-.102	-.095	.041	-.023
level of probability of sign	.75	.99	.92	.9995	.99995	.999	.9995	.991
M_2-M_4 vs. h_2								
best fit slope	-167.	-1.57	17.8	58.8	-22.1	-9.35	-67.3	-22.8
level of probability of sign	.84	.59	.69	.99995	.97	.67	.99995	

*Sea level at Oaks Creek North was substituted when Garden City Pier values were unavailable.

When sea level rises in a typical low-lying shallow estuary, the area submerged intertidally may increase rapidly. Therefore an alternate approach to modeling the effect of rising seas on a shallow inlet-lagoon system such as Murrells is to add progressively more intertidal flats to the model system. Figure 11 shows one-dimensional model results for the behavior of sea surface M_4/M_2 as A_f/A_c increases along the Murrells "average" channel. If A_f/A_c is on the order of 0.68 (the value for the northern system at Murrells), M_4/M_2 decreases with added flats (Figure 11a). At some intermediate A_f/A_c, a change in reponse of M_4/M_2 should be seen. Such a reversal is suggested by a small rise in M_4/M_2 at Garden City Bridge at the highest ocean levels (Figure 10a). But if $A_f/A_c = 1.82$ (the value for the southern system at Murrells), M_4/M_2 increases with added flats. Thus according to both field observations and the model results, an increased area of intertidal flats may account for a significant positive relationship between offshore sea level and estuarine sea surface M_4/M_2. Modeling of sea surface $2M_2$-M_4 does not show a reversal with increased A_f/Ac, only a change in slope (Figure 11b). Yet model velocity results do show a slight reversal in trend at high A_f/A_c (Figures 11c, 11d). The Speer-Aubrey numerical model suggests that seasonal ocean level rise at Murrells may involve a more complex interaction between sea height and tidal flat effects.

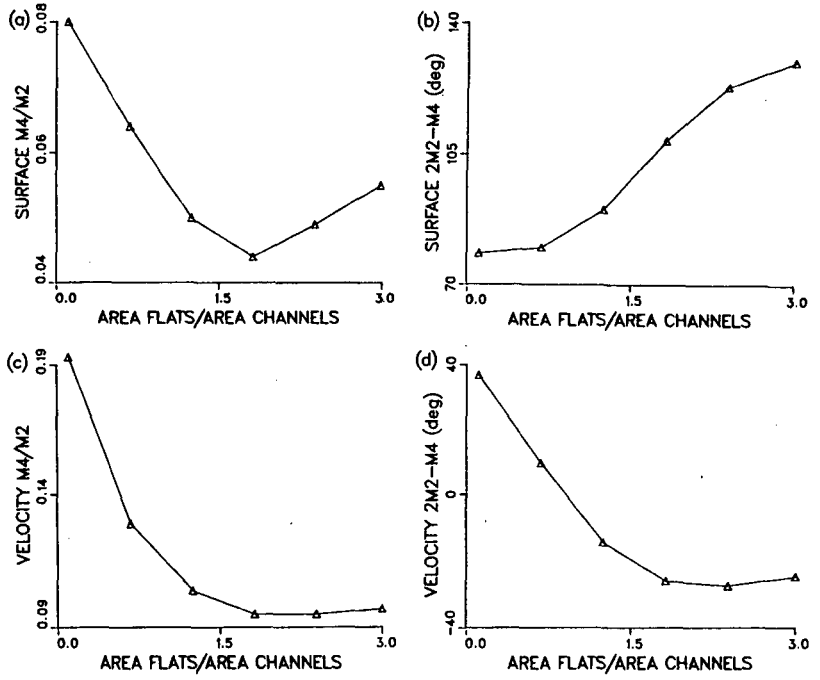

Figure 11. Results of one-dimensional numerical modeling for six model channels differing only in extent of tidal flats (b_0=108m, b_1=59m, h_1=1.9m, h_2=2.6m, l=6.5km, gauge at 6km).

CONCLUSIONS

a) In systems such as Murrells, an estuary having a large tidal amplitude-to-channel depth ratio (a/h), little fresh water input, and moderate tidal flat extent, significant overtides develop from the dominant offshore equilibrium tidal constituents. Where direct measurements of tidal velocities are unavailable, observations of harmonic components of tidal height along with one-dimensional numerical modeling can provide a useful first approximation of distortions in tidal velocity. The primary interaction at Murrells is with the M_2 tide, whose first harmonic, M_4, dominates the non-linear signature of the estuary. Growth of M_4 at Murrells Inlet, as measured by the M_4/M_2 sea surface ratio, directly reflects the degree of tidal distortion within the estuary.

b) Depending upon the relative phase relationships between M_4 and M_2, an estuary will have either floods or ebbs of consistently shorter duration. Within the tidal channels at Murrells, the sea surface $2M_2$-M_4 relative phase is about 90 degrees, leading to a "flood dominant" system having a shorter duration flood tide. Quarter-diurnal tides within Murrells Inlet other than M_4 are also locked in sea surface phase approximately 90 degrees from their respective sources, confirming that M_4 is an accurate sample of non-linear tidal distortion.

c) Tidal distortion differs in the two main channel systems at Murrells. Physical measurements of the estuary and results of numerical modeling both suggest that the concentration of intertidal flats may be the parameter most strongly distinguishing non-linear behavior in the two major channels. Along the channel with a higher concentration of tidal flats, the M_2 sea surface amplitude and the M_4/M_2 ratio are decreased, whereas the M_2 phase lag and the $2M_2$-M_4 relative sea surface phase are greater. Numerical modeling results suggest larger flats also cause M_2 velocity to increase and $2M_2$-M_4 relative velocity phase to decrease.

d) Variations in tidal amplitude over the spring-neap cycle allow the effects of changing a/h to be analyzed. Measurements within Murrells Inlet and numerical modeling results suggest that in flood dominant estuaries such as Murrells, increased tidal amplitude enhances flood dominant nature as reflected by increases in the M_4/M_2 ratio, decreases in the $2M_2$-M_4 relative surface phase, and movement of $2M_2$-M_4 velocity phase toward zero degrees.

e) Insight into the probable impact of accelerated global sea-level rise can be observed directly at Murrells utilizing the steric response to ocean-level change. Measurements within Murrells Inlet and numerical modeling suggest that in areas of moderate tidal flat extent the degree of flood dominance increases with greater tidal amplitude and/or lower sea level as reflected by increases in the M_4/M_2 ratio and decreases in the $2M_2$-M_4 relative sea surface phase; in areas of sufficiently extreme tidal flat concentration the responses of M_4/M_2 and $2M_2$-M_4 phase to changes in sea level are reversed locally.

ACKNOWLEDGMENTS

This work was supported by NOAA National Office of Sea Grant under grant NA79AA-D-0102 and NA80AA-D-0007, Woods Hole Oceanographic Institution Sea Grant Project Number R/B-2, the Waterways Experiment Station's Coastal Engineering Research Center, the Naval Civil Engineering Laboratory, and the Woods Hole Oceanographic Institution's Coastal Research Center. J.D. Boon provided the hourly-averaged tide data for Murrells. J.D. Milliman and E.Uchupi provided comments on an early draft of the manuscript. Contribution number 6644 of the Woods Hole Oceanographic Institution.

REFERENCES

Aubrey, D. G., 1986. Hydrodynamic controls on sediment transport in well-mixed bays and estuaries. In: van de Kreeke, J. (ed.), Physics of Shallow Estuarie and Bays. Springer-Verlag, New York, p. 245-258.

Aubrey, D. G. and Speer, P. E., 1985. A study of non-linear tidal propagation in shallow inlet/estuarine systems. Part I: Observations. Est.. Coast. Shelf Sci., 21:185-205.

Boon, J.D. and Byrne, R.J., 1981. On basin hypsometry and the morphodynamic response of coastal inlet systems. Marine Geology, 40:27-48.

Boothroyd, J. C., 1969. Hydraulic conditions controlling the the formation of estuarine bedforms. In: Hayes, M.O. (ed.), Coastal Environments; N.E. Massachusetts and New Hampshire. Cont. No. 1-CRG, Univ. Massachusetts, Dept. of Geology Publication Series, Amherst, MA, p. 417-427.

Dronkers, J. J., 1964. Tidal Computations in Rivers and Coastel Waters. North Holland Publishing, Amsterdam, 516 pp.

Dronkers, J.J., 1986. Tidal asymmetry and estuarine morphology. Neth. J. Sea Res., 20:117-131.

DuBar, J. R., Johnson, H.S., Thom, B. and Hatchell, W.O., 1974. Neogene stratigraphy and morphology, south flank of the Cape Fear Arch, North and South Carolina. In: Oaks, R. Q. and DuBar, J. R. (eds.), Post-Miocene Stratigraphy: Central and Southern Atlantic Coastal Plain. Utah State Univ. Press, Logan, Utah, p. 140-173.

Emery, K. O., 1967. Estuaries and lagoons in relation to continental shelves. In: Lauff, G. H. (ed.), Estuaries. Amer. Assoc. Adv. Sci., Publ. 83, Washington, DC, p. 9-11.

Friedrichs, C. T. and Aubrey, D. G., in press. Non-linear tidal distortion in shallow well-mixed estuaries: a synthesis. Est. Coast Shelf Sci.

Fry, V.A., 1987. Tidal Velocity Asymmetries and Bedload Transport in Shallow Water Embayments. M.S. thesis, WHOI-MIT Joint Program in Oceanography, Woods Hole, MA, 50 pp.

Hoffman, J. S., Keyes, D. and Titus, J. G., 1983. Projecting Future Sea Level Rise, Methodology, Estimates to the Year 2100, and Research Needs. U.S. EPA 230-09-007, 121 pp.

Masch, F. D., Brandes, R. J. and Reagan, J. D., 1977. Comparison of numerical and physical hydraulic models, Mansonboro Inlet, North Carolina. Apendix 2, v. 1, Numerical Simulation of Hydrodynamics (WRE). GITI Report 6, U.S. Army Coastal Eng. Res. Cent., 123 pp.

National Research Council (NRC), 1979. Carbon Dioxide and Climate: A Scientific Assessment. National Academy Press, Washington, DC, 496 pp.

National Ocean Service, 1984. Index of tide stations: United States of America and miscellaneous other locations. National Oceanic and Atmospheric Administration, 140 pp.

Perry, F. C., Seabergh, W. C. and Lane, E. F., 1978. Improvements for Murrells Inlet, South Carolina. U.S. Army Engineer District, Charleston, and U.S. Army Engineer Waterways Experiment Station, Vicksburg, Mississipi. Technical Report H-78-4, 339 pp.

Postma, H., 1967. Sediment transport and sedimentation in the marine environment. In: Lauff, G. H. (ed.), Estuaries. Amer. Assoc. Adv. Sci., Publ. 83, Washington, DC, p. 158-179.

Richards, H. G., 1974. Structural and stratigraphic framework of the Atlantic Coastal Plain. In: Oaks, R. Q. and DuBar, J. R. (eds.), Post-Miocent Stratigraphy: Central and Southern Atlantic Coastal Plain. Utah State Univ. Press, Logan, Utah, p. 10-20.

Speer, P. E. and Aubrey, D. G., 1985. A study of non-linear tidal propagation in shallow inlet/estuarine systems. Part II: Theory. Est. Coast. Shelf Sci., 21:207-224.